ELSEVIER

23 June 1995

Chemical Physics Letters 240 (1995) 10–16

CHEMICAL PHYSICS LETTERS

Electronic transition moment of the AlO($B\ ^2\Sigma^+$–$X\ ^2\Sigma^+$) emission. Analysis of the R dependence of the $Al^{2+}O^{2-}$ character in the $X\ ^2\Sigma^+$ state

Noriko Sato [a], Haruhiko Ito [a], Kozo Kuchitsu [b]

[a] *Department of Chemistry, Nagaoka University of Technology, Nagaoka 940-21, Japan*
[b] *Department of Chemistry, Faculty of Science, Josai University, Sakado 350-02, Japan*

Received 22 March 1995; in final form 10 April 1995

Abstract

The dependence of the electronic transition moment, $R_e(R)$, of the AlO($B\ ^2\Sigma^+$–$X\ ^2\Sigma^+$) system on the internuclear distance, R, has been determined by an analysis of the intensity distribution of the emission spectra as $R_e(R) = [1 - 2.29(13)(R/\text{Å} - 1.5)^2]$ (1.510 Å $\leqslant R \leqslant$ 1.836 Å). The R dependences of $R_e(R)$ and the $X\ ^2\Sigma^+ \sim A\ ^2\Pi_i$ off-diagonal spin–orbit interaction matrix element, $H_{el}^{SO}(R)$, have been analyzed simultaneously to evaluate the R dependence of the $Al^{2+}O^{2-}$ character in the $X\ ^2\Sigma^+$ state and that of the orbital exponent of the oxygen atom. The results agree with the theoretical prediction by Lengsfield and Liu (J. Chem. Phys. 77 (1982) 6083) that the charge-transfer process, $Al^{2+}O^{2-} \rightarrow Al^+O^-$, takes place in the range of 1.6 Å $\lesssim R \lesssim$ 2.1 Å.

1. Introduction

Extensive studies have been made on the electronic states of the AlO radical [1–17]. Analyses of the transitions extending from the near-infrared to the ultraviolet regions have provided precise molecular constants for the $X\ ^2\Sigma^+$, $A\ ^2\Pi_i$, $B\ ^2\Sigma^+$, $C\ ^2\Pi_r$, and higher electronic states [1–9]. Recently, quite accurate molecular constants for $X\ ^2\Sigma^+$ have been determined from the observations of the microwave transitions [10–12]. These electronic states and relevant transitions have been studied by ab initio calculations [18–22], by which the electronic structures for these states have been discussed in detail.

Among the observed electronic transitions, the $B\ ^2\Sigma^+$–$X\ ^2\Sigma^+$ (blue–green) transition is known to be the most prominent. From a recent analysis of this transition, the molecular constants for $X\ ^2\Sigma^+$ and $B\ ^2\Sigma^+$ have been determined up to $v_X = 7$ and $v_B = 11$ [5].

Contrary to the extensive spectroscopic studies of the $B\ ^2\Sigma^+$–$X\ ^2\Sigma^+$ transition, only limited studies have been reported on the dependence of the electronic transition moment, R_e, on the internuclear distance, R. It has been pointed out in Ref. [21] that the observed R dependences [13–17] are mutually inconsistent and that none of them agrees with the theoretical predictions.

The present study reports on the redetermination of the R dependence of $R_e(R)$. According to the recommendation made by Whiting et al. [23], a rotationally resolved AlO($B\ ^2\Sigma^+$–$X\ ^2\Sigma^+$) emission spectrum is analyzed using the accurate Rydberg–Klein–Rees (RKR) potentials of $X\ ^2\Sigma^+$ and $B\ ^2\Sigma^+$

SSDI 0009-2614(95)00495-5

based on the best available molecular constants for these states [5].

The off-diagonal spin–orbit interaction between the $X\ ^2\Sigma^+$ and $A\ ^2\Pi_i$ states, $H_{el}^{SO}(R)$, has been determined [24] from an analysis of the spin–rotation constant, γ_v, for the $X\ ^2\Sigma^+$, $v = 0$–2 levels [12,13] and the spin–orbit perturbation constant, α, for the $X\ ^2\Sigma^+$, $v = 9 \sim A\ ^2\Pi_i$, $v = 4$ local perturbation [9]. The R dependence of $H_{el}^{SO}(R)$ has been interpreted in terms of the change of the electronic structure in the $X\ ^2\Sigma^+$ state [20]; the charge-transfer process, $Al^{2+}O^{2-} \rightarrow Al^{+}O^{-}$, takes place in the region of 1.6 Å $\lesssim R \lesssim$ 2.1 Å. In the present study, a similar interpretation is applied to the R dependence of $R_e(R)$. A simultaneous analysis of $R_e(R)$ and $H_{el}^{SO}(R)$ is made to provide the R dependences of the $Al^{2+}O^{2-}$ character in the $X\ ^2\Sigma^+$ state and the orbital exponent of the $2p_0$ Slater-type orbital (STO) function of the oxygen atom.

2. Experimental

The AlO($B\ ^2\Sigma^+$–$X\ ^2\Sigma^+$) emission was produced by a microwave discharge (2.45 GHz, 80 W) of a mixture of $AlCl_3$ vapor, oxygen, and argon in a flow cell [2]. The pyrex glass cell was made of a discharge tube of 15 mm diameter, a stainless steel nozzle of 1 mm diameter, a quartz observation window, and an evacuation section (Fig. 1). The $AlCl_3$ vapor was generated by resistive heating of solid anhydrous $AlCl_3$ to $\approx$ 140°C. A trace amount of O_2 was added through the nozzle. The total pressure in the cell was about 1 Torr. The emission was monitored through the window as shown in Fig. 1, where the deposition of Al_2O_3 powder was negligible. The discharge area was separated from the anhydrous $AlCl_3$ sample in order to prevent the Al_2O_3 powder from coating the surface of $AlCl_3$. With this experimental setup, an intense and stable blue–green emission due to the AlO($B\ ^2\Sigma^+$–$X\ ^2\Sigma^+$) transition was observed for several hours. The emission spectrum was measured by a Jovin-Yvon THR-1500 monochromator in the double-pass mode. The intensity of the emission was monitored by an electronically cooled photomultiplier tube (Hamamatsu R2949). The observed signal was processed by a photon-counter (Stanford SR400). The spectral intensity was calibrated using a standard halogen lamp (Ushio Electric).

3. Results and analysis

3.1. Observed spectra

The vibronic bands, $(v_B, v_X) = (0, 0–1), (1, 0–2)$ and $(2, 0–4)$, were observed. When the rotational lines were fully resolved, as shown in Fig. 2, the intensities of the rotational lines originating from the same (v', N') levels were compared directly to evaluate the relative values of the electronic transition moments for the two vibronic levels. When the rotational lines were overlapped with one another, the relative values of the electronic transition moments were evaluated by a simulation analysis of the observed spectra: For instance, the 1–2 band is overlapped with the 0–1 band, as shown in Fig. 3a; hence the contribution of this band was taken into account in the simulation analysis, as shown in Fig. 3b. The relative value of $R_e(R)$ for the 1–2 band was evaluated by simulating the observed spectrum of the 1–0 band taken under the same experimental conditions, as described below.

3.2. Analysis

The relative values of $R_e(R)$ are evaluated by the following analysis. The intensity of the rotational

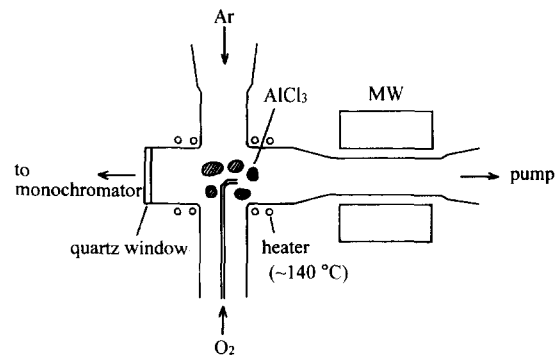

Fig. 1. Schematic view of the flow cell for the observation of the AlO($B\ ^2\Sigma^+$–$X\ ^2\Sigma^+$) emission.

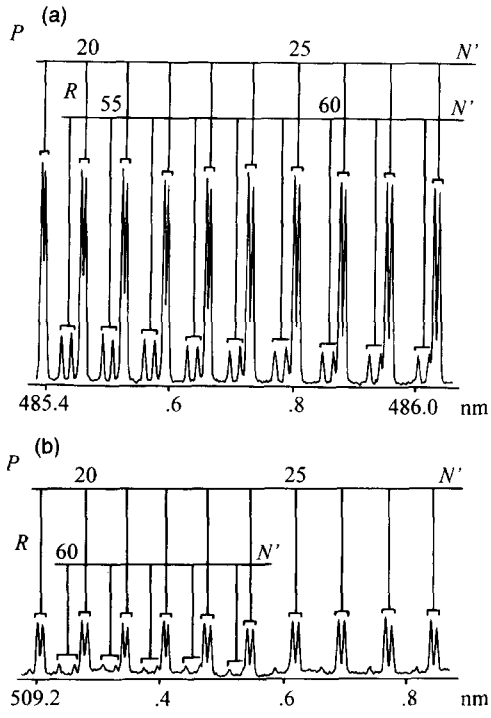

Fig. 2. Observed spectra of the AlO(B $^2\Sigma^+$–X $^2\Sigma^+$) (a) 0–0 and (b) 0–1 bands.

line, $I_{v''N''}^{v'N'}$, originating from the (v', N')–(v'', N'') transition is expressed as

$$I_{v''N''}^{v'N'} \propto P_{v'N'}\left[\nu_{v''N''}^{v'N'}\right]^3\left[(R_e)_{v'v''}\right]^2 S_{N''}^{N'} S_e\left(\nu_{v''N''}^{v'N'}\right), \quad (1)$$

where $P_{v'N'}$ is the rovibrational population, $\nu_{v''N''}^{v'N'}$ is the transition wavenumber, $S_{N''}^{N'}$ is the Hönl–London factor, and $S_e(\nu_{v''N''}^{v'N'})$ is the sensitivity of the detection system.

(i) When the rotational lines in the v'–v'' and v'–u'' bands are fully resolved, the ratio of the square of the vibrational matrix elements of the electronic transition moments,

$$\left[(R_e)_{v'v''}/(R_e)_{v'v''}\right]^2 = \left[\langle v' \mid R_e(R) \mid v''\rangle / \langle v' \mid R_e(R) \mid u''\rangle\right]^2, \quad (2)$$

is evaluated by comparing the intensities of the individual rotational lines corresponding to the (v', N')–(v'', N'') and (v', N')–(u'', N'') transitions as

$$I_{v''N''}^{v'N'}/I_{u''N''}^{v'N'} \propto \left[\nu_{v''N''}^{v'N'}/\nu_{u''N''}^{v'N'}\right]^3\left[(R_e)_{v'v''}/(R_e)_{v'u''}\right]^2 \times\left[S_e\left(\nu_{v''N''}^{v'N'}\right)/S_e\left(\nu_{u''N''}^{v'N'}\right)\right], \quad (3)$$

by which $[(R_e)_{v'v''}/(R_e)_{v'u''}]^2$ can be evaluated independently of $P_{v'N'}$ and $S_{N''}^{N'}$. Since spectral overlaps are confirmed to be negligible for the rotational lines of $N' \approx 19$–32 in the v'–v'' bands for $v' = 0$–2, $v'' = 0$ and 1, the intensities of these lines are used to evaluate $[(R_e)_{v'v''}/(R_e)_{v'u''}]^2$.

(ii) When the rotational lines are overlapped with those of other vibronic bands, a simulation analysis is made for the observed spectrum as follows: The molecular constants for the B $^2\Sigma^+$ and X $^2\Sigma^+$ states are taken from Ref. [15], and $P_{v'N'}$ is approximated by a Boltzmann distribution as

$$P_{v'N'} \propto (2N'+1)\left[\exp(-E_{rot}/kT_{rot})\right], \quad (4)$$

where k is the Boltzmann constant. The rotational energy of the v'th vibrational level of the B $^2\Sigma^+$ state is expressed as

$$E_{rot} = B_{v'}N'(N'+1) - D_{v'}\left[N'(N'+1)\right]^2, \quad (5)$$

where $B_{v'}$ and $D_{v'}$ are the rotational and second-order centrifugal distortion constants, respectively, for the

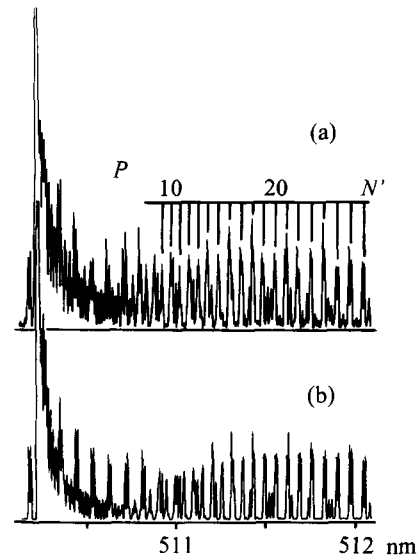

Fig. 3. (a) Observed and (b) simulated spectra of the AlO(B $^2\Sigma^+$–X $^2\Sigma^+$) 2–1 band.

Table 1
Vibrational matrix elements of the AlO($B\,^2\Sigma^+ - X\,^2\Sigma^+$) transition moment

v' [a]	v'' [b]	u'' [b]	$[(R_e)_{v'v''}/(R_e)_{v'u''}]^2$ [c]	Obs. − calc. [d]
0	1	0	0.295(16) [e]	−0.004
1	0	1	0.771(33) [e]	−0.006
2	0	1	0.178(11) [e]	0.026
1	0	2	0.838[16] [f]	−0.004
2	0	3	0.145[13] [f]	−0.012
2	0	4	0.618[53] [f]	−0.007

[a] Vibrational quantum number of AlO($B\,^2\Sigma^+$).
[b] Vibrational quantum number of AlO($X\,^2\Sigma^+$).
[c] Observed values.
[d] Calculated values are based on Eq. (8).
[e] Determined by analyzing the ratios of individual rotational lines. See Section 3.2. Values in parentheses denote standard errors.
[f] Determined by spectral simulation. See Section 3.2. Values in brackets denote estimated errors.

$B\,^2\Sigma^+$ state [5]. The effective rotational temperatures, T_{rot}, and their limits of error are estimated to be 550 ± 50, 450 ± 30, and 390 ± 30 K for the $v' = 0$, 1 and 2 levels, respectively, by a simulation analysis of the bands in which the overlaps are negligible. A part of the observed spectra, particularly the high N' region of the R-branch and the very low N' region of the P- and R-branches, cannot be reproduced by a single Boltzmann distribution (see Figs. 3a and 3b). However, the intensities of the rotational lines in these N' regions do not make significant influence on the relative intensities of the (v', v'') and (v', u'') bands: A simulation analysis is made on the band heads and the band envelopes, to which the middle N' region ($10 \lesssim N' \lesssim 30$) contributes dominantly, to determine the $[(R_e)_{v'v''}/(R_e)_{v'u''}]^2$ values listed in Table 1 and on the relative intensities of the overlapping bands (see Fig. 3b) [1]. The errors in the $[(R_e)_{v'v''}/(R_e)_{v'u''}]^2$ values are found to originate mainly from those in the T_{rot} values estimated above. These ratios are used to evaluate the relative values of $R_e(R)$.

3.3. Determination of $R_e(R)$

The relative values of $R_e(R)$ are determined by an analysis of the $[(R_e)_{v'v''}/(R_e)_{v'u''}]^2$ values listed in Table 1 as follows: $R_e(R)$ is expressed as

$$R_e(R) = 1 + a_1(R - R_0) + a_2(R - R_0)^2 + \ldots, \tag{6}$$

where a_i ($i = 1, 2, \ldots$) are adjustable parameters and R_0 is a fixed parameter which is optimized by trial and error. The vibrational matrix elements of $R_e(R)$ are then expressed as

$$(R_e)_{v'v''} = \langle v' \mid v'' \rangle + a_1(\langle v' \mid R \mid v'' \rangle - R_0\langle v' \mid v'' \rangle) + a_2(\langle v' \mid R^2 \mid v'' \rangle - 2R_0\langle v' \mid R \mid v'' \rangle + R_0^2\langle v' \mid v'' \rangle) + \ldots . \tag{7}$$

The values of the vibrational integrals, $\langle v' \mid R^n \mid v'' \rangle$ ($n = 0, 1, 2, \ldots$), are evaluated using the RKR potentials of the $B\,^2\Sigma^+$ and $X\,^2\Sigma^+$ states based on the reported molecular constants for these states [5]. When only the a_2 value is adjusted, with a_1 and R_0 fixed at 0 and 1.5 Å, respectively, the $[(R_e)_{v'v''}/(R_e)_{v'u''}]^2$ values can be fitted satisfactorily; the result of the fitting is

$$a_2 = -2.29(13)\ \text{Å}^{-2}, \tag{8}$$

and the standard deviation, σ, is estimated to be 0.013. The effective range of R is evaluated from the r-centroids, $\langle v' \mid R \mid v'' \rangle / \langle v' \mid v'' \rangle$, of the transition observed in the present study as

$$1.510\ \text{Å} \leqslant R \leqslant 1.836\ \text{Å}. \tag{9}$$

Larger values of σ are obtained when other functional forms of $R_e(R)$ are chosen: For example, $\sigma = 0.028$ is obtained when R_0 is chosen to be 1.6 Å, and $\sigma = 0.015$ when the first-order polynomial is assumed for $R_e(R)$. When a_1 and a_2 are both adjusted simultaneously, a strong correlation between them is indicated.

[1] In this simulation analysis, the caluculated relative intensities of the F_1 and F_2 components are found to be reversed in comparison with the observed spectrum (see, for example, the P(20) transition in Fig. 3). This reversal has also been pointed out by Launila and Jonsson [8]. It is probably due to the reversed sign of γ_v for the $B\,^2\Sigma^+$ state. However, the differences in the intensities of the F_1 and F_2 components are so small that this reversal does not influence the results of the present analysis.

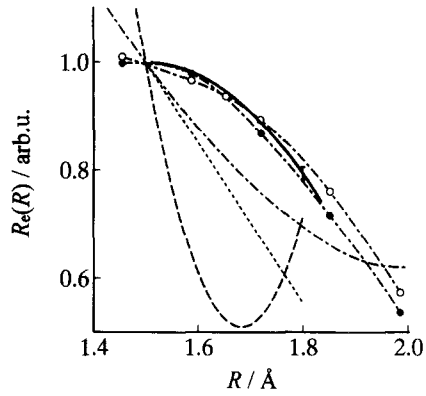

Fig. 4. Variations of the electronic transition moment of the AlO($B\,^2\Sigma^+ - X\,^2\Sigma^+$) system with the internuclear distance, R, normalized at $R = 1.5$ Å. (———) Present study; error bar denotes standard deviation; (●---●, ○---○) ab initio calculations using different basis sets [21]; (-----) ab initio calculation [22], (- - - - -) experimental [14], (– – –) experimental [17].

4. Discussion

4.1. R dependence of $R_e(R)$

The R dependence of $R_e(R)$ determined in the present study is compared in Fig. 4 with the reported dependences [14,17,21,22] normalized at $R = 1.5$ Å. The present R dependence is found to be in much better agreement than the previous experimental results [15,17] with the theoretical dependences predicted by Partridge et al. [21], which is much more accurate than the predictions by Kovba and Topol [22].

The present R dependence is claimed to be more accurate than the previous experimental reports by Hébert and Tyte [14] and by Hébert et al. [17]: (i) The relative intensities measured in the present study are based on the measurement carried out with much higher resolution than the previous measurements [14,17], and (ii) the RKR potentials used in the present analysis are more reliable than those used in the previous studies, because the present potentials are based on the best available molecular constants for $B\,^2\Sigma^+$ and $X\,^2\Sigma^+$ [5].

4.2. Electronic structure of AlO($X\,^2\Sigma^+$)

The transfer from $Al^{2+}O^{2-}$ to Al^+O^- is predicted to take place in the region of $1.6\ \text{Å} \lesssim R \lesssim 2.1$ Å [20]. This region overlaps closely with the range of R where $R_e(R)$ is significant (see Eq. (9)). In the subsequent analysis, the R dependence of the $Al^{2+}O^{2-}$ character in the $X\,^2\Sigma^+$ state is evaluated by a simultaneous analysis of $R_e(R)$ determined in the present study and the off-diagonal spin–orbit interaction, $H_{el}^{SO}(R)$, between the $X\,^2\Sigma^+$ and $A\,^2\Pi_i$ states,

$$H_{el}^{SO}(R)/\text{cm}^{-1} = 53.35(95) - 162.0(3.0)\left(R/\text{Å} - 1.9\right) \quad (1.6\ \text{Å} \leqslant R \leqslant 1.9\ \text{Å}), \tag{10}$$

determined in Ref. [24]. The electronic wavefunction of $X\,^2\Sigma^+$, $|X\,^2\Sigma^+(R)\rangle$, is approximated as

$$|X\,^2\Sigma^+(R)\rangle = c(R)\,|\text{II}\rangle = d(R)\,|\text{I}\rangle, \tag{11}$$

where $|\text{I}\rangle$ and $|\text{II}\rangle$ are the wavefunctions corresponding to the Al^+O^- and $Al^{2+}O^{2-}$ structures, respectively, and $c(R)$ is assumed to be real and positive. From the normalization condition, $d(R)$ is expressed as

$$d(R) = -c(R)S \pm \left[1 + (S^2 - 1)c(R)^2\right]^{1/2}, \tag{12}$$

where S is the overlap integral, $\langle \text{I}|\text{II}\rangle$; the choice of the double sign is discussed later. Since the $B\,^2\Sigma^+$ state has predominantly the Al^+O^- character [18,19], the $R_e(R)$ function for the $B\,^2\Sigma^+ - X\,^2\Sigma^+$ transition normalized at $R = 1.5$ Å is approximated in terms of the transition between the Al^+O^- structure in $B\,^2\Sigma^+$ and the $Al^{2+}O^{2-}$ structure in $X\,^2\Sigma^+$ as

$$R_e(R) = c(R)\langle B|\,\mu_z\,|\text{II}\rangle / c_0\langle B|\,\mu_z\,|\text{II}\rangle_0, \tag{13}$$

where $|B\rangle$ is the wavefunction of $B\,^2\Sigma^+$, μ_z is the z component of the transition-moment operator, and the subscript 0 denotes the values at $R = 1.5$ Å. Similarly, $H_{el}^{SO}(R)$ is approximated in terms of the off-diagonal spin–orbit interaction for the Al^+O^- structure [24],

$$H_{el}^{SO}(R) = -2^{-1/2}d(R)\zeta(O^-), \tag{14}$$

because the $A\,^2\Pi_i$ state has predominantly the Al^+O^- structure [18,19]. In Eq. (14), the minus sign is required for the inverted nature of the $X\,^2\Sigma^+ \sim A\,^2\Pi_i$ spin–orbit interaction [24], and $\zeta(O^-)$ is assumed to be 121 cm^{-1} [25]. The matrix ele-

ments, $\langle B | \mu_z | \mathrm{II} \rangle$ and S, can be reduced to the one-electron integrals between the atomic orbitals relevant to the transition as

$$\langle B | \mu_z | \mathrm{II} \rangle \approx -\langle 3s(\mathrm{Al}) | \mu_z | 2p_0(\mathrm{O}) \rangle \quad (15)$$

and

$$S \approx -\langle 3s(\mathrm{Al}) | 2p_0(\mathrm{O}) \rangle, \quad (16)$$

where the minus signs are due to the bonding nature of the 3s(Al)–$2p_0$(O) bond. The matrix elements appearing in Eqs. (15) and (16) are obtained analytically in terms of the elliptical coordinates by use of the STO functions, where right-handed coordinates are used for the Al and O atoms and the value of the orbital exponent of the 3s atomic orbital of aluminium, $\zeta_{3s}(\mathrm{Al})$, is assumed to be 1.027212 [20]. Eq. (16) gives $S > 0$. This provides the reasoning that the double sign in Eq. (12) should be chosen as positive: When $c(R) = 1$, Eq. (12) gives $d(R) = 0$ if the plus sign is chosen, and the $X\ ^2\Sigma^+$ state has predominantly the Al^+O^- character at large R as expected [20], whereas an alternative choice gives $d(R) = -2S\ (\neq 0)$.

The $R_e(R)$ and $H_{el}^{SO}(R)$ values are solved for individual values of R using Eqs. (12)–(14) to evaluate the $|c(R)|^2$ value and the orbital exponent of oxygen, $\zeta_{2p_0}(\mathrm{O})$, as shown in Fig. 5. The $|c(R)|^2$ value in Fig. 5a decreases rapidly from ≈ 0.94 at $R = 1.6$ Å to ≈ 0.56 at $R = 1.8$ Å. This suggests that the AlO($X\ ^2\Sigma^+$) state has predominantly the $Al^{2+}O^{2-}$ structure at $R = 1.6$ Å and approximately a 1:1 mixture of the $Al^{2+}O^{2-}$ and Al^+O^- structures at $R = 1.8$ Å, being in good agreement with the theoretical prediction [20]. Fig. 5b shows that the $\zeta_{2p_0}(\mathrm{O})$ value varies from ≈ 0.52 at $R = 1.6$ Å to ≈ 0.98 at $R = 1.8$ Å. These values correspond well with the $\zeta_{2p_0}(\mathrm{O})$ values used in the calculation of Lengsfield and Liu, 0.40831 and 0.86393 [20]. The positive R dependence of $\zeta_{2p_0}(\mathrm{O})$ shown in Fig. 5b also suggests the $Al^{2+}O^{2-} \rightarrow Al^+O^-$ charge-transfer process as R increases [20].

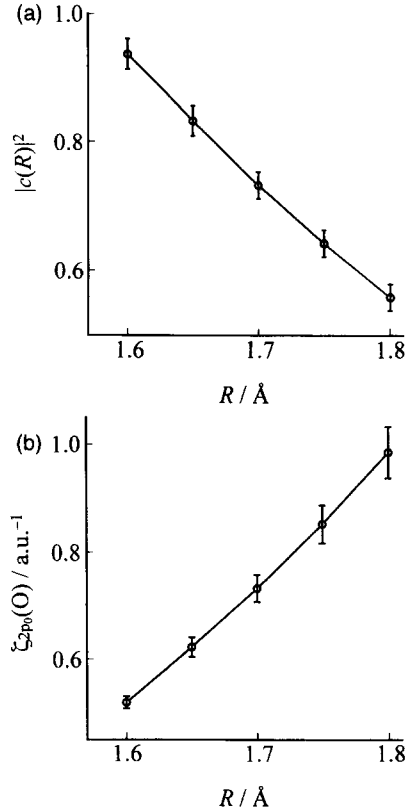

Fig. 5. (a) Coefficient of the $Al^{2+}O^{2-}$ character in the AlO ($X\ ^2\Sigma^+$) state; see Eq. (11). (b) Orbital exponent of the $2p_0$ Slater-type function of the O atom in the AlO ($X\ ^2\Sigma^+$) state. (○) Evaluated as described in Section 4.2, where error bar denotes standard deviation. (–) Interpolated.

5. Conclusion

The R dependence of R_e, determined more accurately than in previous experimental studies, agrees well with the theoretical prediction by Partridge et al. [21]. A simultaneous analysis of $R_e(R)$ and $H_{el}^{SO}(R)$ provides detailed experimental information on the electronic structure of an ionic radical, AlO.

Acknowledgement

The authors thank Mr. Tsutomu Tojo for his development of the program for spectral simulation and Mr. Kei-ichi Namiki for his helpful discussion. The RKR potentials and the vibrational matrix elements were calculated at the Computer Center of the Institute for Molecular Science (IMS). This work has been supported by the Joint-Studies Program of IMS (1994).

References

[1] W.C. Pomeroy, Phys. Rev. 29 (1927)59.
[2] J.K. McDonald and K.K. Innes, J. Mol. Spectry. 32 (1969) 501.
[3] M. Singh, G.V. Zope and S.L.N.G. Krishnamachari, J. Phys. B 18 (1985) 1743.
[4] J.A. Coxon and S. Naxakis, J. Mol. Spectry. 111 (1985) 102.
[5] M.D. Saksena, G.S. Ghodgaonkar and M. Singh, J. Phys. B 22 (1989) 1993.
[6] J.P. Towle, A.M. James, O.L. Bourne and B. Simard, J. Mol. Spectry. 163 (1994) 300.
[7] J.P. Towle, A.M. James, O.L. Bourne, B. Simard, M. Singh and M.D. Saksena, J. Mol. Spectry. 167 (1994) 472.
[8] O. Launila and J. Jonsson, J. Mol. Spectry. 168 (1994) 1.
[9] H. Ito, Can. J. Phys. 72 (1994) 1082.
[10] T. Törring and R. Herrmann, Mol. Phys. 68 (1989) 1379.
[11] C. Yamada, E.A. Cohen, M. Fujitake and E. Hirota, J. Chem. Phys. 92 (1990) 2146.
[12] M. Goto, S. Takano, S. Yamamoto, H. Ito and S. Saito, Chem. Phys. Letters 227 (1994) 287.
[13] N.R. Tawde and V.M. Korwar, Proc. Natl. Inst. Sci. India 29A (1963) 325.
[14] G.R. Hébert and D.C. Tyte, Proc. Phys. Soc. 83 (1964) 629.
[15] D.C. Tyte and G.R. Hébert, Proc. Phys. Soc. 84 (1964) 830.
[16] C. Linton and R.W. Nicholls, J. Quant. Spectry. Radiative Transfer 9 (1969) 1.
[17] G.R. Hébert, R.W. Nicholls and C. Linton, J. Quant. Spectry. Radiative Transfer 23 (1980) 229.
[18] J. Schamps, Chem. Phys. 2 (1973) 352.
[19] M. Yoshimine, A.D. McLean and B. Liu, J. Chem. Phys. 58 (1973) 4412.
[20] B.H. Lengsfield III and B. Liu, J. Chem. Phys. 77 (1982) 6083.
[21] H. Partridge, S.R. Langhoff, B.H. Lengsfield III and B. Liu, J. Quant. Spectry. Radiative Transfer 30 (1983) 449.
[22] V.M. Kovba and I.A. Topol, J. Mol. Struct. THEOCHEM 137 (1986) 65.
[23] E.E. Whiting, A. Schadee, J.B. Tatum, J.T. Hougen and R.W. Nicholls, J. Mol. Spectry. 80 (1980) 249.
[24] H. Ito and M. Goto, Chem. Phys. Letters 227 (1994) 293.
[25] H. Lefebvre-Brion and R.W. Field, Perturbations in the spectra of diatomic molecules (Academic Press, New York, 1986).